Use of Infrared Spectroscopy To Characterize Clay Intercalation and Exfoliation in Polymer Nanocomposites

Kenneth C. Cole*

National Research Council Canada, Industrial Materials Institute, 75 De Mortagne Blvd., Boucherville, Quebec, Canada J4B 6Y4

Received December 11, 2006; Revised Manuscript Received November 19, 2007

ABSTRACT: The use of infrared spectroscopy as a technique for characterizing the state of intercalation and exfoliation in polymer nanocomposites prepared from montmorillonite-based nanoclays was investigated. The nanocomposite samples were based on polypropylene (blown films) or high-density polyethylene (extruded material). It was clearly shown that the shape of the clay band envelope in the 1350−750 cm^{-1} region, which includes four Si−O stretching modes, varies with the degree of processing and is sensitive to the quality of intercalation/exfoliation. Peak fitting was used to elucidate the nature of the changes and to develop quantitative indicators. The out-of-plane Si−O mode near 1070 cm^{-1} is particularly sensitive and undergoes significant changes. Infrared spectroscopy is a valuable complement to established techniques like X-ray diffraction and transmission electron microscopy and has the added advantage of being able to provide a relatively fast indication of the overall degree of intercalation/exfoliation, including clay particles with interlayer spacings outside the range of X-ray diffraction. Furthermore, it offers the possibility of use as a quality control method, either in the laboratory or on-line.

Introduction

Polymer nanocomposites based on layered silicate reinforcement materials continue to attract considerable attention. These reinforcements, which may be naturally occurring (for example, montmorillonite clay) or synthetic, possess a structure consisting of negatively charged aluminosilicate layers less than 1 nm thick, closely associated in stacks, with counterbalancing cations like sodium along with loosely bound water molecules located in the space between the layers. By appropriate treatment, the metal cations can be replaced by larger organic ions (intercalants) that increase somewhat the interlayer distance. The most common intercalants are quaternary ammonium ions bearing at least one relatively long hydrocarbon chain. When such organoclays are dispersed in a polymer or a polymer precursor, further intercalation can occur and in ideal circumstances will lead to complete separation of the layers or exfoliation. The result is a very efficient reinforcing effect because the layers are highly anisometric (1 nm thick and hundreds of nm in diameter) and a relatively small amount of clay can give rise to a very large number of particles with a correspondingly large surface area. Consequently, less than 5 wt % of clay can produce significant improvements in various properties (mechanical, barrier, fire retardancy, etc.) with little adverse effect on transparency and density.

Since the improvements in properties are directly related to the quality of clay intercalation and exfoliation, it is important to properly characterize the degree of layer separation. The two techniques commonly used for this purpose are X-ray diffraction (XRD) at small angles ($2\theta < 10°$) and transmission electron microscopy (TEM). Both provide useful information, but even together they do not give a complete picture. XRD data typically show a peak whose position is related to the interlayer spacing d_{001} through the Bragg relationship $d_{001} = \lambda/(2 \sin \theta)$. The peak maximum thus corresponds to the most probable spacing, and its broadness can give some idea of the distribution of spacings, although it is also related to other factors. Careful sample preparation, experimental technique, and data interpretation are necessary if reliable information is to be obtained from XRD.[1] One disadvantage of XRD is the fact that data cannot be obtained at 2θ angles of less than about 1°, which corresponds to d_{001} around 8 nm. Thus, XRD "sees" only intercalated clay and not exfoliated clay and gives little indication of the relative amounts of each type. Transmission electron microscopy, on the other hand, gives a more direct visual indication of the state of the clay, including individual exfoliated layers and intercalated stacks.[2,3] This gives a good qualitative picture, but to have a more quantitative overall measure of a sample, it is necessary to perform a statistical average over a large number of analyses, a very time-consuming and expensive process.

Infrared (IR) spectroscopy is extensively used to characterize a wide range of materials, including layered silicates.[4−7] It is surprising therefore that its use for characterizing nanoclay exfoliation seems to have been so little explored. We recently published a study in which IR spectroscopy was used to quantify the degree of orientation of both the polypropylene matrix and the reinforcing clay in blown nanocomposite films.[8] In the course of that work, we became aware of the potential of this technique for obtaining information on the state of exfoliation in nanocomposites, and the purpose of this paper is to report our results on these films as well as on other samples that we subsequently examined. To our knowledge, there has been only one other report of similar findings.[9]

Layered silicates present a rather complicated subject for IR analysis.[4−7] The silicon−oxygen stretching vibrational modes give rise to strongly absorbing bands in the 1100−1000 cm^{-1} region. Some of these involve the basal oxygens of the silicon−oxygen tetrahedra, i.e., they correspond to Si−O−Si linkages at the surface of the clay layers and have their transition moment (the direction of dipole oscillation during the vibration) lying in the plane of the layer; they are thus designated "in-plane". Others involve the apical oxygens, i.e., they correspond to the $Si-O^-$ bonds directed toward the octahedrally coordinated

* E-mail: kenneth.cole@imi.cnrc-nrc.gc.ca.

10.1021/ma0628329 CCC: $40.75 Published 2008 by the American Chemical Society
Published on Web 12/29/2007

aluminum ions at the center of the layer; these vibrations have their transition moment perpendicular to the layer and are designated "out-of-plane". The intrinsically high absorptivity of these bands results in significant variations in the refractive index in this region, and consequently when the clays are dispersed in a supporting medium for analysis, reflection at the clay−medium interface can complicate the spectrum and affect the overall band shape. Farmer and Russell have described how the spectrum depends on the type of clay as well as on the particle size and structure.[4−7] In the case of Wyoming montmorillonite, for example, they observed four overlapping bands: three in-plane (1120, 1048, 1025 cm^{-1}) and one out-of-plane (1080 cm^{-1}).[5] They reported that the position and sharpness of the out-of-plane mode "varies surprisingly with physical state". For instance, it is particularly sensitive to particle size and shows significant apparent shifts when the crystals are thinner than 100 nm. They attributed this behavior to the strong electric field produced by the oscillating $Si-O^-$ dipoles, which causes the thin plates of the layer silicate crystals to become electrically polarized like the dielectric in a parallel-plate condenser.[6,10] Furthermore, Russell and Farmer used IR spectroscopy to study the dehydration of montmorillonite and saponite via the water O−H stretching band around 3700−3000 cm^{-1} and the H−O−H bending band at 1640−1630 cm^{-1}.[11] They were able to distinguish two types of interlayer water, namely "firmly held" water molecules directly coordinated to the exchangeable cations and more labile water molecules in outer spheres of coordination. Thus, changes in the interlayer spacing related to the loss of water could be correlated with IR results, and the shape of the Si−O stretching band envelope was also found to be affected. The swelling of clays with water was later studied in detail by Low and co-workers.[12−16] Lerot and Low studied different montmorillonites swollen to varying degrees and examined the effect on the shape of the Si−O stretching absorption.[12] They found that (i) the frequencies of the four component peaks depended on the type of montmorillonite (degree of isomorphous substitution), but not on the water content; (ii) the out-of-plane mode became much more prominent with increasing water content, and the in-plane modes became narrower and more intense; (iii) the absorption coefficient for the principal Si−O absorption decreased with increasing isomorphous substitution but increased with increasing water content; and (iv) there was a rather abrupt change at a certain critical degree of swelling, which they attributed to a sudden rearrangement of the particles. For Upton montmorillonite with lithium or sodium as the interlayer cation, Zhang and Low established a clear linear correlation between the interlayer spacing, as measured by XRD, and the mass ratio of water to clay, m_w/m_c.[13] The position of the water H−O−H bending vibration was later shown to also vary with m_w/m_c.[14] In a related study,[15] the Si−O band envelope was analyzed in detail with the use of peak fitting to decompose it into four components: peak I (~1115 cm^{-1}), peak II (the out-of-plane mode, ~1080 cm^{-1}), peak III (~1045 cm^{-1}), and peak IV (~1024 cm^{-1}). The envelope clearly changes shape as m_w/m_c is varied from 0.71 (58% clay) to 42.8 (2% clay). Peak II, which can be barely seen at the lower water contents, becomes very visible as the interlayer spacing increases. In addition, the intensity ratio of peak III to peak IV increases. The positions of all four peaks shift as a function of m_w/m_c, but the greatest shift is observed for peak II. The changes reach a plateau at $m_w/m_c \cong 6$, the point at which the spontaneous swelling of montmorillonite ceases and the interlayer distance is about 15 nm. It is interesting to note that this is well beyond the range that can be detected by XRD (about 8 nm). When water was replaced by NaCl or LiCl solutions of varying concentrations, no significant effect was observed.[16] However, in a recent study in which the Fe^{3+} in the montmorillonite was reduced to Fe^{2+}, it was found that the iron oxidation state exerted a profound influence on the relationship between the water content and the position of the Si−O component peaks and that the effect was reversible.[17]

Given these observations for water, similar behavior might be expected for other "swelling" media. In fact, such effects have been reported for hydrocarbon oil in a paper proposing the use of IR for characterizing the extent of dispersion of an organo-clay complex in the oil.[18] It is therefore not surprising to find that it can also be applied to polymers, as will be demonstrated in this paper.

Experimental Section

The following nanoclays were obtained from Southern Clay Products, Inc.: Cloisite Na^+ (sodium montmorillonite, X-ray d_{001} 1.17 nm); Cloisite 10A (intercalated with 39 wt % dimethyl benzyl hydrogenated tallow quaternary ammonium, d_{001} 1.92 nm); Cloisite 15A (intercalated with 43 wt % dimethyl di(hydrogenated tallow) quaternary ammonium, d_{001} 3.15 nm); Cloisite 20A (same intercalant at 38 wt %, d_{001} 2.42 nm); and Cloisite 30B (intercalated with 30 wt % methyl tallow bis-2-hydroxyethyl quaternary ammonium, d_{001} 1.85 nm). Nanomer I.30E (intercalated with 25−30 wt % octadecylamine) and Nanomer I.28E (25−30 wt % trimethylstearyl ammonium) were obtained from Nanocor, Inc.

Blown polypropylene (PP) films with and without nanoclay and compatibilizing agent were prepared and analyzed as described elsewhere.[8] The constituents were polypropylene homopolymer (Pro-fax PDC1274 from Basell Polyolefins), Cloisite 15A at a level of 2 wt %, and the following two maleic anhydride-grafted polypropylene (MAgPP) compatibilizing agents: Epolene 43 from Eastman Chemical Co., with a low molecular weight ($M_w = 9000$) but high MA content (3.8 wt %), and Polybond 3150 from Chemtura Corp., with a high molecular weight ($M_w = 330\,000$) and low MA content (0.5 wt %).

Blends of high-density polyethylene (HDPE, Sclair 2714 from Nova Chemicals) and maleic anhydride-grafted HDPE (Polybond 3009 from Chemtura Corp.) were prepared from cryogenically ground starting materials by processing at 190 °C in a Haake "Minilab" twin-screw microextruder. The processed blends were also cryogenically ground. Nanocomposites containing 2 wt % of Cloisite 20A were made from dry blends of the nanoclay with the ground blends or neat polymers, also by processing in the Haake extruder at 190 °C. To obtain products with different states of intercalation/exfoliation, the materials were recirculated in the extruder for different periods of time ranging from 0 min (one pass straight through) to 30 min. Thin films for IR analysis and thicker samples for X-ray diffraction analysis were prepared by rapid hot pressing of the extrudate.

Infrared spectra were recorded on a Nicolet Magna 860 FT-IR instrument from Thermo Electron Corp. (DTGS detector, resolution 2 cm^{-1}, accumulation of 128 scans). Diffuse reflection spectra were measured with a "praying mantis" accessory from Harrick Scientific Corp. Peak fitting was performed with the use of GRAMS/AI software from Thermo Galactic Corp.

Results and Discussion

If the shape of the clay Si−O band envelope is to be considered for use as an indicator of clay intercalation in a polymeric matrix, it is first important to determine as a reference the spectrum for the clay in its initial unintercalated and undispersed state, with as little perturbation as possible. This was done in two ways. In the first, the clay is dispersed in Nujol mineral oil by light hand mixing with a mortar and pestle at room temperature, the mixture is sandwiched between potassium

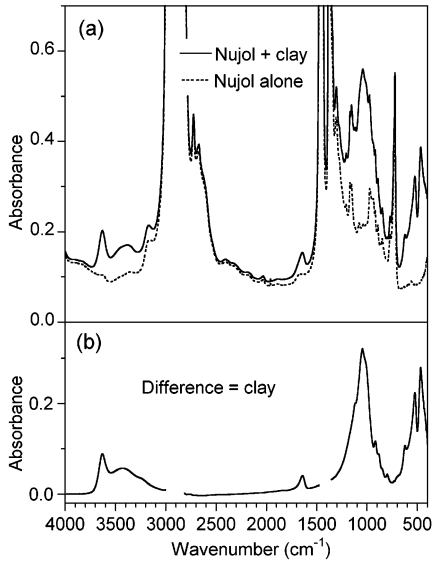

Figure 1. (a) IR transmission spectrum of Nujol containing 2 wt % of Cloisite Na^+ sodium montmorillonite clay (solid line) and the spectrum of Nujol alone (dotted line). (b) Difference spectrum obtained by subtraction, showing the clay absorption peaks. The blank spaces correspond to regions where the Nujol peaks are saturated.

bromide windows with a 100 μm spacer, and the IR spectrum is measured in transmission. After the spectrum is converted to absorbance units, the Nujol peaks are eliminated by subtracting the spectrum of pure Nujol obtained in the same way. The result for 2 wt % Cloisite Na^+ (sodium montmorillonite) is shown in Figure 1. The difference spectrum clearly shows the usual montmorillonite absorption peaks, and the baseline is close to zero. In the second method, the clay is again hand mixed in a mortar and pestle, but this time with potassium bromide powder, and the spectrum is measured in diffuse reflection mode and ratioed against that of neat KBr. According to theory, after conversion to Kubelka−Munk units of $(1 - R)^2/2R$, where R is the reflectance, the result should resemble the absorbance spectrum.

To check the effect of concentration, spectra of Cloisite Na^+ were measured by both methods at different concentrations. The resulting spectra in the Si−O stretching region are shown in Figure 2, both as recorded (Figure 2a,b) and normalized to unit peak height to compare the band shapes (Figure 2c,d). In Figure 2c, the four Si−O stretching modes are labeled I, II, III, and IV following the convention of Yan et al.[15] (Peak II is not obvious because of overlap by the others.) The weaker peaks at 915, 880, and 845 cm^{-1} are librational modes of hydroxyl ions associated with two cations in the central octahedral layer, arising respectively from Al_2OH, $Fe^{3+}AlOH$, and MgAlOH groupings.[4] The origin of the peak at 798 cm^{-1} is uncertain. In transmission, up to 4% concentration the overall band shape changes little, but at 6% it changes somewhat. In diffuse reflection, the band shape is constant up to 2% but deviates significantly at 4% and 6%. In Figure 3, the peak heights are plotted against concentration for both methods. The relationship is linear up to 2%, but deviations are observed at 4% and 6%, especially for diffuse reflection. We conclude that concentration effects are important but can be minimized if transmission spectra are run at 4% or less and diffuse reflection spectra at 2% or less. However, even at these low levels, there is a significant difference between the transmission spectra and the diffuse reflection spectra. Although the peaks occur at much the same frequencies, the band envelope has a different shape and is noticeably narrower in diffuse reflection than in transmission. This is probably because of the different way in which reflection effects influence the spectra of these heterogeneous samples. Because the Si−O vibrations have very high intrinsic absorptivity, the refractive index in this region can be quite high, giving rise to a significant amount of reflection at the interface between the particles and the medium. This can lead to multiple reflections within the sample, meaning that the effective path length is not constant. In transmission spectra, this is known to lead to an apparent "flattening" of peaks, a phenomenon sometimes known as the "wedging effect" because it occurs when the two faces of a sample or cell are not parallel.[19]

Figure 4 compares the spectra of several different nanoclays measured in both transmission (2% in Nujol) and diffuse reflection (1% in KBr). The same trend is observed in both cases, namely, a significant narrowing of the band envelope upon the introduction of organic intercalant between the clay layers of the sodium montmorillonite. In the case of the Cloisite clays, peaks I and III can be seen at 1120 and 1045 cm^{-1}, respectively, with peak IV as a shoulder near 1015 cm^{-1}. In the case of the Nanomer clays, the shape of the envelope is significantly different; peaks I, III, and IV have all shifted downward by about 10 cm^{-1}, whereas peak II has shifted upward and can now be seen more clearly around 1085 cm^{-1}. This difference can very probably be attributed to the different origins of the two montmorillonites. The peak at 880 cm^{-1} is noticeably weaker in the Nanomers than in the Cloisites, which suggests that the Nanomers contain a lower amount of Fe^{3+}. This would explain the differences in the overall band shape because Yan and Stucki observed exactly the same changes when the Fe^{3+} ions in sodium-saturated Upton montmorillonite were reduced to Fe^{2+}.[17] Figure 4 confirms that the Si−O stretching band envelope is affected by both the chemistry of the montmorillonite and the presence of intercalant.

It is well-known that orientation can also profoundly affect the band shape because the intensity of the IR absorption is proportional to the square of the dot product of the vectors corresponding to the transition moment of the vibration and the electric field of the radiation, i.e., to the square of the cosine of the angle between the two. Thus, if the clay layers are aligned perpendicular to the IR beam direction, the in-plane modes (peaks I, III, and IV) will be enhanced while the out-of-plane mode (peak II) will be diminished.[4] This can be clearly seen in Figure 5, taken from our earlier work on blown PP films containing 2 wt % of the nanoclay Cloisite 15A.[8] It shows the spectra of a film with the composition 78% PP, 2% Cloisite 15A, and 20% of the compatibilizing agent Polybond 3150. The spectra labeled "MD" and "TD" were measured with the film perpendicular to the beam and with polarization in the machine direction and the transverse direction, respectively. Because of strong clay layer orientation in the plane of the film, the in-plane modes III and IV are quite strong while the out-of-plane mode II is very weak. The spectrum labeled "ND" corresponds to polarization in the normal or thickness direction of the film. Since the spectrum cannot be easily measured with the film turned by 90° with respect to the beam, the ND spectrum is obtained by tilting the film at 45° and then correcting for the contribution of the MD or TD spectrum. The ND spectrum is quite different from the MD and TD spectra; the out-of-plane mode is now quite prominent while the in-plane modes are very weak. The structural factor spectrum SF is obtained by taking the average of the other three. It corresponds to the spectrum that would be obtained if there were no orientation in the sample. It should be noted that measuring the spectrum without polarization does not give the SF spectrum; instead, it gives

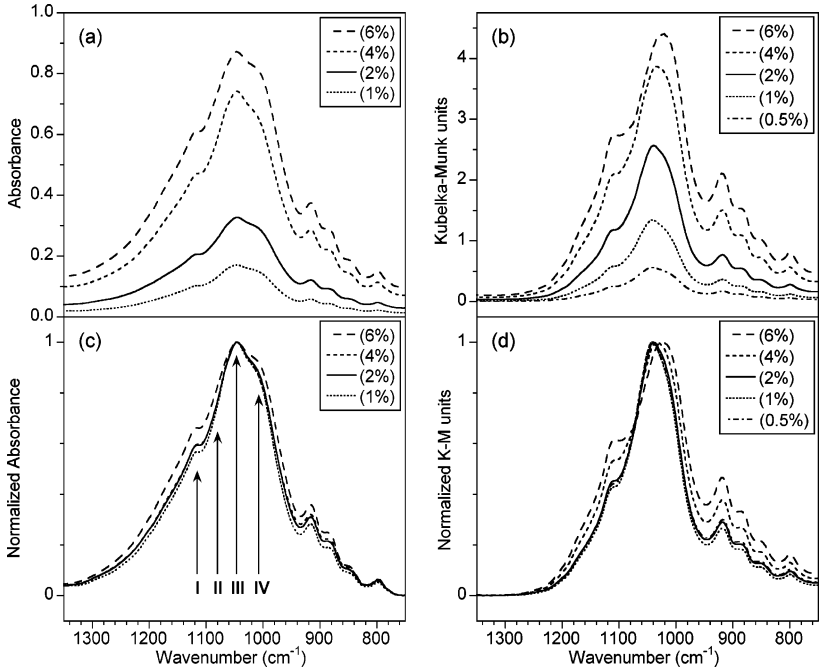

Figure 2. IR spectra in the Si−O stretching region of Cloisite Na^+ (sodium montmorillonite) clay: (a) spectra measured in transmission at different concentrations in Nujol, after subtraction of the Nujol spectrum; (b) spectra measured in diffuse reflection at different concentrations in KBr powder; (c) transmission spectra normalized to unit peak height; (d) diffuse reflection spectra normalized to unit peak height.

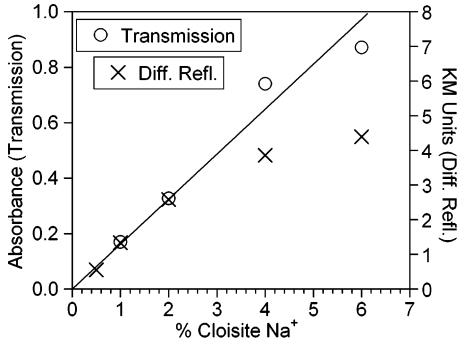

Figure 3. Relationship between peak height and concentration for the spectra of Figure 2.

the average of the MD and TD spectra, which can be quite different.

In our earlier publication, we considered only the orientation in the blown films and did not report on other aspects. We now consider the structural factor spectra of the different films, which are free of orientation effects. These are shown in Figure 6 along with the spectrum of Cloisite 15A dispersed by hand in Nujol for comparison. The thickness of the films was such that the measured absorbance never exceeded 1.1 below 1350 cm^{-1}. To better see the clay peaks, the spectrum of the PP matrix has been subtracted in the same way described for Nujol. In the case of PP, the subtraction sometimes leaves small residual features, probably because of slight crystallinity differences. Interference fringes also appear in some spectra. However, the variations in the shape of the clay band envelope are clearly evident. Compared to the unprocessed clay (Figure 6a), clay that has been processed with PP in the extruder (Figure 6b−f) gives a narrower band envelope and shows a visible peak II. Even without compatibilizing agent, this peak can be seen at 1075 cm^{-1} (Figure 6b). When 4% Epolene 43 is present in the composition, it becomes more obvious and the maximum shifts to 1077 cm^{-1} (Figure 6c). With 4% Polybond 3150 instead of Epolene 43, it becomes still more obvious and shifts to 1079 cm^{-1} (Figure 6d). The trend continues if the concentration of Polybond is increased, with peak II continuing to shift slightly to 1080 cm^{-1} (Figure 6e) and 1081 cm^{-1} (Figure 6f). This apparent growth and/or shift of peak II is very similar to that observed for swelling with water.[15] It seems reasonable, therefore, to associate this trend with increasing efficiency of intercalation/exfoliation, and the XRD data included in Figure 6 tend to support this to a certain extent. If we consider only the PP films with Polybond concentrations of 0, 4, 20, and 38%, the trend is clear (d_{001} = 2.8, 3.2, 4.0, and 4.0 nm) and follows the IR results. The results for the starting clay and the film containing Epolene do not follow the IR trend exactly, however. One possible explanation for this is that the chemistry of the intercalant has an influence on the spectrum. Although Epolene and Polybond are both MAgPPs, Epolene has much higher MA content and much lower molecular weight. Another possible cause is the difficulty in correlating the XRD and IR data. It must be remembered that the clay layer spacing is by no means uniform but is distributed over a wide range of values, possibly including the state of complete exfoliation. The maximum of the XRD curve is a measure only of the most probable spacing, and while the shape of the curve gives some idea of the distribution, XRD cannot give reliable data below 2θ about 1° or $d_{001} > 8$ nm. The IR response, on the other hand, is an average over all the clay present, including particles beyond the range of XRD. For this reason, it would be a more reliable indicator of the overall extent of intercalation/exfoliation.

To explore the potential of IR analysis in greater depth, a more systematic study was undertaken on high-density polyethylene (HDPE), the maleated HDPE Polybond 3009, and blends thereof with Polybond contents of 1, 2, 33, and 67 wt %. As described in the Experimental Section, Cloisite 20A nanoclay was dispersed in each matrix at a level of 2 wt % in a microextruder at 190 °C for different processing times, and from the extrudate, thick and thin films were prepared by rapid hot pressing for XRD and IR analysis, respectively. Unlike the blown films, these pressed films were analyzed without polarization and tilting to correct for orientation effects, as this would have required considerable extra effort. A few of the films

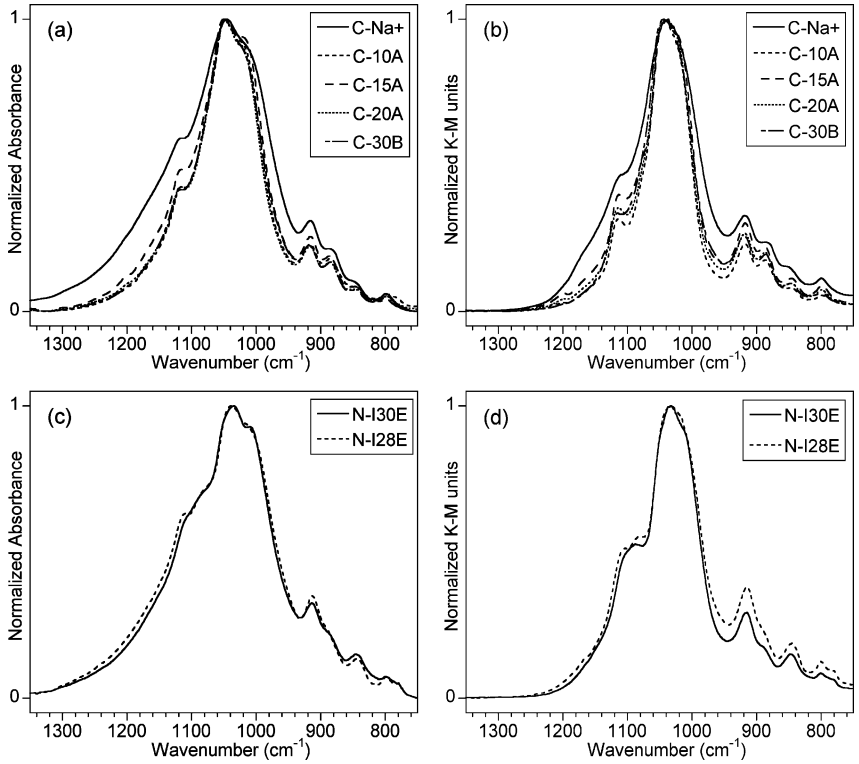

Figure 4. IR spectra of different clays, normalized to unit peak height for comparison: (a) Cloisite clays at 2% in Nujol, transmission; (b) Cloisite clays at 1% in KBr, diffuse reflection; (c) Nanomer clays at 2% in Nujol, transmission; (d) Nanomer clays at 1% in KBr, diffuse reflection.

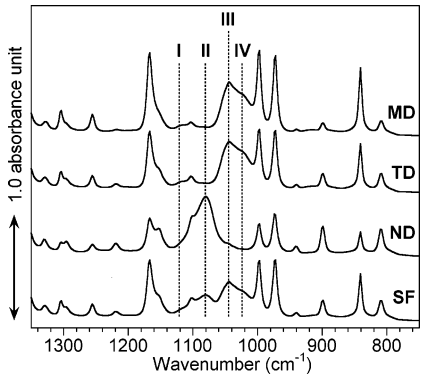

Figure 5. IR spectra (offset along the *y*-axis for clarity) of a blown PP nanocomposite film corresponding to polarization in the machine direction (MD), the transverse direction (TD), and the normal direction (ND), along with the structural factor spectrum (SF). Peaks I to IV are the Si−O stretching modes of the clay.

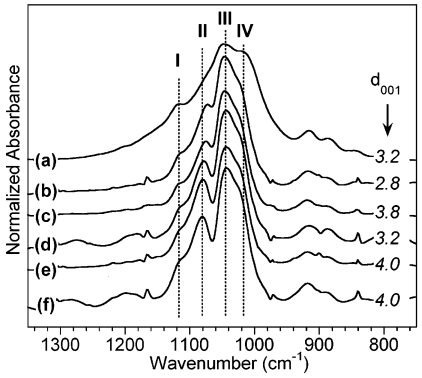

Figure 6. IR spectra of 2% Cloisite 15A: (a) dispersed by hand in Nujol; (b−f) in PP nanocomposite films containing different compatibilizing agents: (b) none; (c) 4% Epolene 43; (d) 4% Polybond 3150; (e) 20% Polybond 3150; (f) 38% Polybond 3150. The interlayer spacings d_{001} (in nm) corresponding to the maxima of the peaks in the XRD curves are shown on the right.

were analyzed in this way, and although it was found that the pressing induced some clay orientation, the degree was significantly lower than in the blown films (Hermans orientation function around 0.3 as compared to 0.8) and fairly reproducible. Hence, it was felt that the orientation effects could be considered as a constant factor that would not interfere with the comparison of the spectra, which are shown for four of the compositions in Figure 7 along with the reference spectrum of Cloisite 20A measured in Nujol. As in the previous examples, the spectrum of the polymer matrix has been subtracted.

The first observation is that, regardless of the matrix composition, just one pass through the microextruder (0 min recirculation) results in substantial narrowing of the band envelope compared to the unprocessed Cloisite 20A (whose envelope is already narrower than that of the unintercalated Cloisite Na^+, as shown in Figure 4). In the case of pure HDPE (Figure 7a), peak II becomes somewhat more evident at this point but does not appear to evolve much more with further recirculation. With 2% Polybond in the PP matrix (Figure 7b), after one pass the spectrum is similar to the one for no Polybond, but after recirculation for 1 min it becomes more prominent and then seems to remain stable. When the Polybond content is 33%, peak II is much more prominent even after one pass and then remains stable. Much the same is true for 100% Polybond. If the IR spectrum is an indication of intercalation/exfoliation, a stable state seems to be attained rather quickly, and although this state depends on the concentration of compatibilizing agent up to a certain level, beyond that there seems to be little effect.

It is obviously of interest to quantify these changes in the clay spectrum so as to be able to compare the state of exfoliation in different samples. This is not an easy task. In an attempt to do so, we have applied peak fitting to the spectra in order to better understand the changes that are occurring, but again, this is not easy. There are always important questions concerning

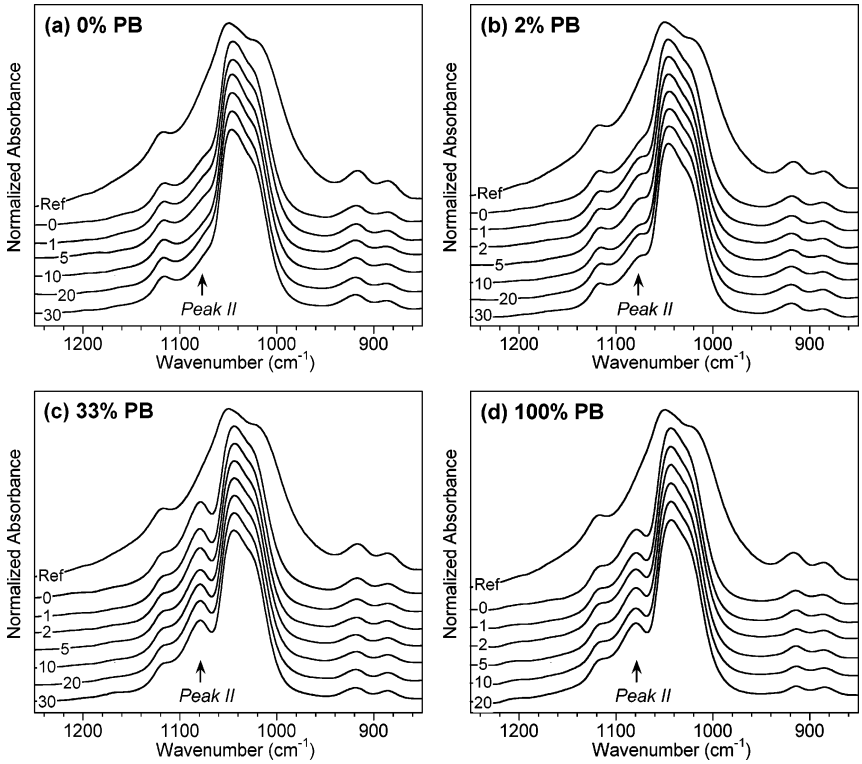

Figure 7. IR spectra of 2% Cloisite 20A dispersed by hand in Nujol ("Ref") or processed in HDPE containing different amounts of Polybond 3009 (indicated at the top left of each graph) for different recirculation times in minutes (indicated at the bottom left of each graph).

the choice of line shape and the number of peaks to use. While the theory-based Lorentzian line shape works well in many cases, like liquids and well-ordered solids, it does not necessarily work so well in the case of a less-well-structured solid like the naturally occurring layered silicates. This is because the clay particles comprise a distribution of structures and environments with slightly different vibrational frequencies, so that the overall IR absorption band can be considered as the superposition of a distribution of Lorentzian peaks. This introduces Gaussian character into the line shape. To deal with this situation, we have used the well-known Pearson VII line shape function,[20,21] which includes an adjustable parameter m that allows the line shape to vary from purely Lorentzian ($m = 1$) to purely Gaussian ($m = \infty$). After trials with a number of spectra, we found $m = 4$ (about 75% Gaussian character) to be the best value for general use. It was assumed that the line shape is the same for all peaks in the spectrum, which is not necessarily entirely true. However, if the line shape is allowed to vary in the fit along with the other parameters (peak position, width, and height), then there are too many variables, and it is impossible to obtain a reliable convergent fit.

Figure 8 shows some results obtained for a typical spectrum (2% Cloisite 20A in 2:1 Polybond:HDPE at 20 min recirculation time). We began with the approach used by Yan et al.,[15] namely fitting the 1160−960 cm^{-1} region with four peaks and a linear variable baseline. Peak fitting in the same region was also successfully applied to spectra of nylon-6 nanocomposites by Loo and Gleason[22] and allowed them to make the interesting observation that the clay peaks III and IV shift to lower frequency when the nanocomposite is subjected to strain. Although this approach served the purposes of those authors quite well, it can be seen from the residual curve in Figure 8a that in the present case there is room for improvement. The fit should really comprise the whole band envelope, including the four weaker peaks at lower wavenumber. When this is done, the best result that could be obtained with eight peaks is shown in Figure 8b. It is clearly inadequate. Using different values of m over the whole range from Lorentzian to Gaussian did not improve the fit significantly, and in fact a Lorentzian line shape gave the worst result. When a ninth peak was added, the best result was obtained with a very broad underlying peak that we designate peak V, as shown in Figure 8c. This is better than Figure 8b, but still inadequate, and again changing the line shape gave no significant improvement. A more reasonable fit was obtained on adding a tenth peak, as shown in Figure 8d. This amounts to splitting peak III into two components, designated peaks IIIa and IIIb. However, the most acceptable fit was obtained with 11 peaks, as shown in Figure 8e, where peak II is also split into two components, peaks IIa and IIb. Thus, in the best fit, peaks II and III seem to consist of two components, and the broad peak V is required. (If peak V is removed from the fit of Figure 8e and the fit repeated, then one of the other peaks moves to replace the broad peak.) It should be stressed that this approach to the peak fitting is not based only on the spectrum shown in Figure 8, but on trials with a large number of spectra measured for different Cloisites processed under different conditions in different polymers and in mineral oil. Although the origin of the "new" peaks is not entirely clear, they represent real effects. In the case of peaks II and III, the two components are probably not different vibrational modes but are required to account for an asymmetry of the peak that arises from an asymmetric distribution of environments in the sample. For peak II, this asymmetry can be seen in the ND spectra of oriented samples, where the peak stands out clearly. It can be seen, for example, in Figure 5, in spite of the presence of the small superimposed PP peak at 1103 cm^{-1}. In our earlier work on orientation,[8] the trichroic spectra were analyzed by peak fitting with the inclusion of peaks IIa, IIb, IIIa, and IIIb. The average respective dichroic ratios A_{par}/A_{perp} for these four peaks in the five films analyzed (which showed similar orientation) were found to be respectively 0.13, 0.05, 2.94, and 2.60, where "parallel" and "perpendicular" refer to the direction of the

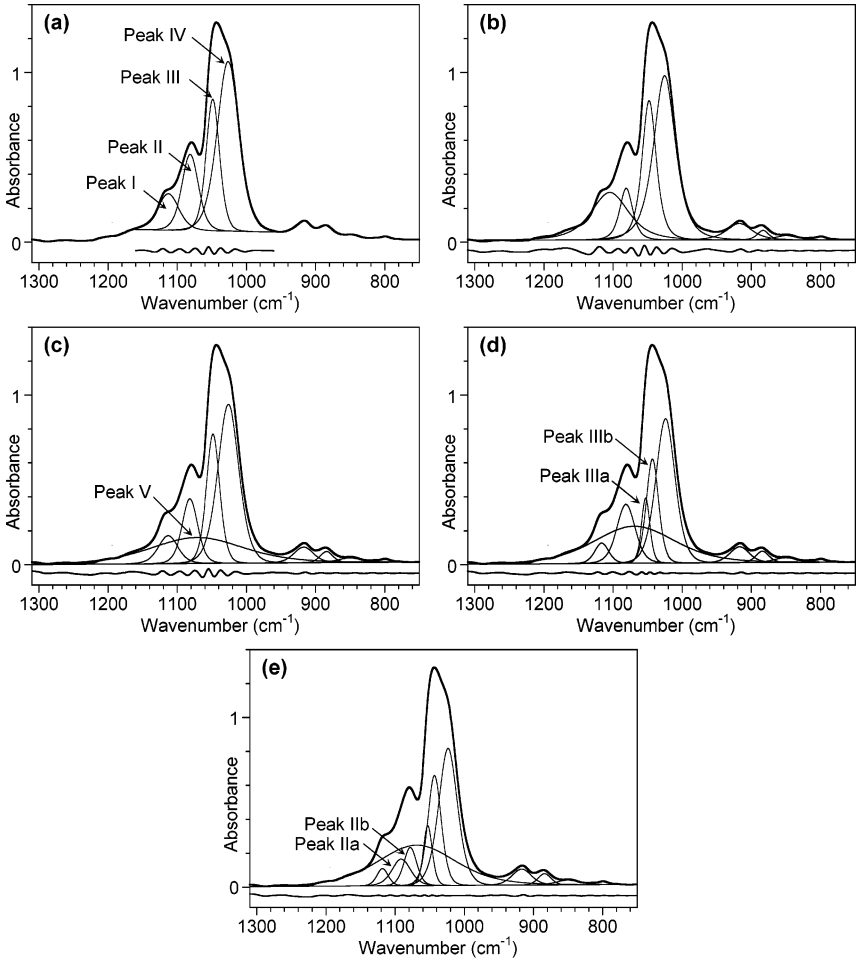

Figure 8. Peak fits of the clay band envelope for 2% Cloisite 20A in 2:1 Polybond:HDPE at 20 min recirculation time: (a) fit with 4 peaks from 1160 to 960 cm^{-1} only; (b) fit of complete band envelope with 8 peaks; (c) fit with 9 peaks; (d) fit with 10 peaks; (e) fit with 11 peaks. The curve of intermediate thickness at the bottom of each graph corresponds to the residual difference between the experimental spectrum (thick line) and the sum of the fitted peaks (thin lines). It is displaced downward from zero for greater visibility.

polarization with respect to the plane of the film. This confirms that both peaks IIa and IIb show similar "out-of-plane" dichroism, whereas peaks IIIa and IIIb show similar "in-plane" dichroism, the opposite of peaks IIa and IIb.

The apparent broad underlying peak V is unfortunately more difficult to explain at this point. It is unlikely that a normal vibrational mode would give rise to a peak of this width, so it appears to be a somewhat empirical means of dealing with the varying broadness of the overall band envelope, the origin of which is not clear. It should be stressed that it was impossible to account for this variation by varying the width or line shape of the other individual peaks, unless an unduly large number of peaks were introduced. One possible explanation for the effect is Mie scattering, which has been reported to produce broad undulating features in the spectra of oral mucosa cells.[23] Another explanation, already mentioned, is the occurrence of reflection at the surface of the clay particles, caused by a difference in the index of refraction, that leads to an effectively nonuniform path length and a "flattening" of the peak shape. If air were entrapped within aggregated clay particles, this effect would be accentuated because the difference in refractive index between clay and air is greater than between clay and Nujol or polymer. To check this, samples of Cloisite Na^+ and Cloisite 20A in Nujol were examined before and after evacuation to remove any entrapped air, but no significant difference was observed. A third explanation is some other optical effect related to the general state of microdispersion of the clay. To check this, a sample of 2 wt % Cloisite 20A in Nujol, mixed by hand

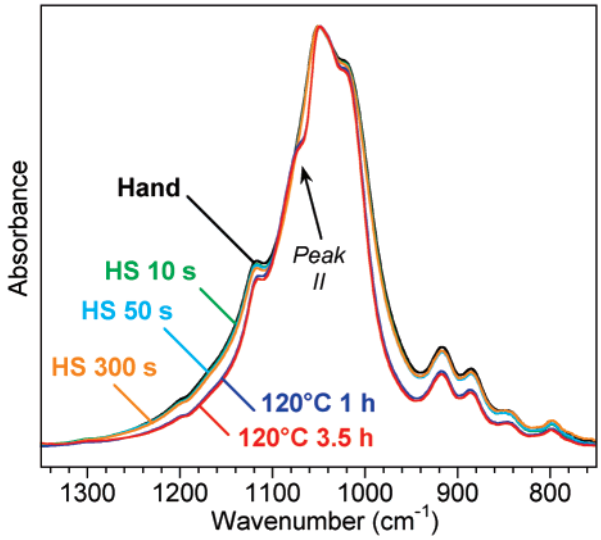

Figure 9. Evolution of the IR spectrum of Cloisite 20A in Nujol at 2 wt % for a mixture as prepared by hand mixing, then after mixing with a high-speed (HS) homogenizer for 10, 50, and 300 s, and then after heating without mixing at 120 °C for 1 and 3.5 h.

(i.e., rather poorly dispersed), was further mixed with a high-speed homogenizer at room temperature for different times up to 5 min to improve the state of dispersion while minimizing intercalation. As shown in Figure 9, the shape of the clay band envelope showed no significant change compared to the hand-

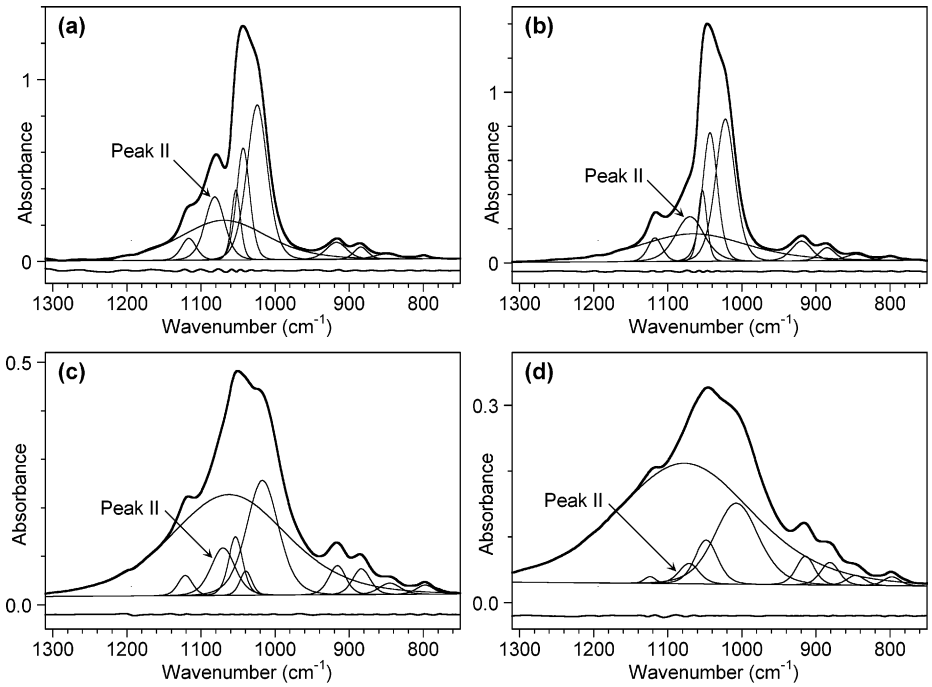

Figure 10. Examples of peak fits of different clay spectra: (a) 2% Cloisite 20A in 2:1 Polybond:HDPE at 20 min recirculation time; (b) 2% Cloisite 20A in HDPE alone at 30 min recirculation time; (c) 2% Cloisite 20A in Nujol; (d) 2% Cloisite Na^+ in Nujol.

mixed sample. However, when the well-dispersed sample was heated at 120 °C, without any further mixing, intercalation of Nujol occurred, and the band shape changed in two respects: it became narrower and peak II became more prominent (Figure 9). This confirms that both the band narrowing and the appearance of peak II are related mainly to the clay intercalation and not to the physical dispersion of the clay at the microscale level. Further evidence for this comes from Figure 4, where a clear difference is seen between the unintercalated clay and the intercalated ones, even though their state of dispersion should be similar. Furthermore, this difference is observed both for Nujol suspensions and for dry mixtures with KBr measured in diffuse reflection. Yet another possible explanation for the broad feature is that it really does arise from a fraction of the clay that gives rise to broader peaks that overlap to form a rather "amorphous" ensemble. Schaefer et al. clearly observed band narrowing similar to that reported here when organo-bentonite was dispersed in mineral oil.[18] They suggested that at low degrees of dispersion/intercalation, where the nanometer-thick clay layers are close together, coupling of vibrations from adjacent layers broadens the IR bands. If this is so, then as the layers are pushed apart by intercalation, this effect would diminish and the band envelope would narrow. In untreated montmorillonite (like Cloisite Na^+), the amount of intercalated water might also vary from one clay gallery to another, affecting the interlayer distance and the coupling and giving rise to a further "blurring" of the spectrum. Whatever the origin of the band narrowing effect, a rigorous explanation is not obvious at this point. The intercalation process is complex and leads to a product with spatial inhomogeneity at the nanometer scale. There may be phenomena involved that will only be fully recognized after further work. However, it is important to recognize this effect in the analysis, and for the time being the best available approach seems to be the use of peak V.

Although the fit with 11 peaks shown in Figure 8e can be successfully used in many cases, this is not always true. Problems arise when peak II does not stand out clearly and is "hidden" under the other peaks. In such cases, peaks IIa and IIb cannot be unequivocally determined by the peak fitting process. Thus, as a general approach, we decided to use a total of 10 peaks, that is, to represent peak II by one component only, even if this is an approximation. Figure 10 compares examples of different spectra analyzed with this approach. Figure 10a is the case already discussed. The "waviness" of the residual curve in the region of peak II confirms that the fit is not perfect with 10 peaks, but nevertheless it is reasonably good. Figure 10b is a spectrum obtained with HDPE alone, where peak II is less evident. In this case, the fit with 10 peaks is better than in Figure 10a, and if an extra peak is added to the fit, problems with convergence result. Figure 10c is the spectrum of Cloisite 20A in Nujol. The much larger overall bandwidth in this case is accounted for by a stronger peak V. Peaks I, II, IIIa, IIIb, and IV are still well determined, although the relative intensities of peaks IIIa and IIIb have changed somewhat. Finally, Figure 10d shows the spectrum of the unintercalated clay Cloisite Na^+, in which the absorption band is quite broad. Nevertheless, the fit still works well, although in this case only one component was required for peak III as well as for peak II.

Having developed this peak fitting protocol, which we stress again was found to work well for a wide variety of clay spectra, we then applied it to the series of spectra shown (in part) in Figure 7. The data were then analyzed closely to determine which parameters are most sensitive to the matrix and the processing. As expected, peak II was particularly sensitive. Both the peak position and the width at half-height change with processing, as shown in Figure 11. For the pure HDPE, the position remains close to that of the starting clay (1070 cm^{-1}) and the peak remains hidden under peaks III and IV. As a result, its position and width are harder to determine with precision, and the variations seen in Figure 11 may not be significant. For the blends containing Polybond, however, the situation is more clear. At 1% Polybond, peak II shifts to 1072.5 cm^{-1} after one pass through the extruder and then to 1074.4 and 1076.4 cm^{-1} after 1 and 2 min, respectively, of recirculation. At this point the system appears to reach a steady state. With 2% Polybond, the changes occur somewhat faster, with the peak shifting to 1076.2 cm^{-1} after only 1 min of recirculation and then reaching a plateau around 1077.1 cm^{-1}, slightly higher than

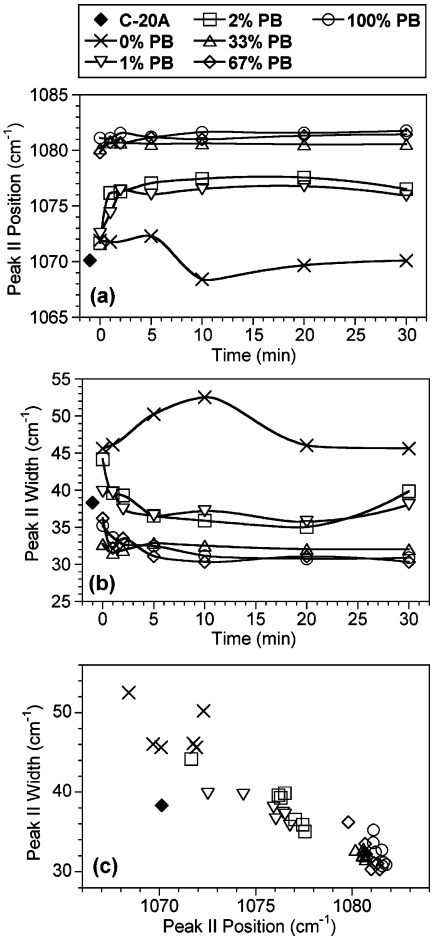

Figure 11. Peak II parameters determined by peak fitting for Cloisite 20A in blends of Polybond 3009 (PB) and HDPE with varying percentages of PB: (a) peak position in cm^{-1} as a function of recirculation time; (b) width at half-height in cm^{-1} as a function of recirculation time; (c) relationship between peak position and width. The legend for the symbols is shown at the top of the figure. The C-20A data point (◆) corresponds to the reference spectrum recorded in Nujol.

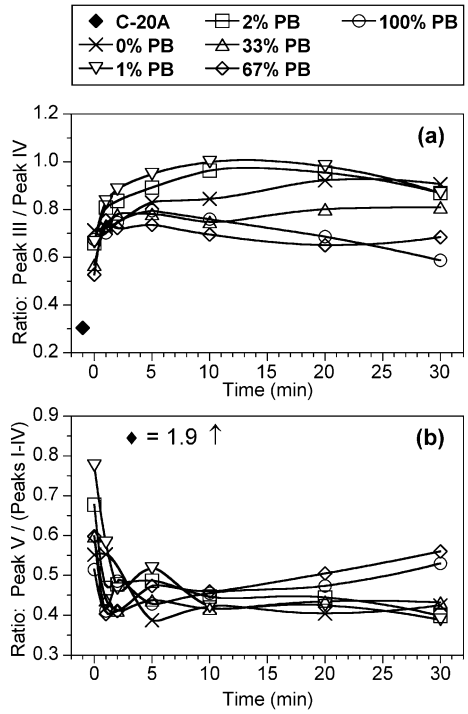

Figure 12. Parameters determined by peak fitting for Cloisite 20A in blends of Polybond 3009 (PB) and HDPE with varying percentages of PB: (a) ratio of the area of peak III with respect to that of peak IV; (b) ratio of the area of the broad underlying peak V with respect to the sum of peaks I−IV. The legend for the symbols is shown at the top of the figure. The C-20A data point (◆) corresponds to the reference spectrum recorded in Nujol.

at 1%. When the Polybond concentration is very high, the steady state is reached after only one pass, and the plateau values are higher still: 1080.6 cm^{-1} at 33% Polybond, 1081.0 cm^{-1} at 67% Polybond, and 1081.5 cm^{-1} at 100% Polybond. It should be noted that these values are the same as those found for high concentrations of compatibilizing agent in the blown PP films. The increase in the frequency of peak II is accompanied by a parallel decrease in the peak width, as shown in Figure 11b. In fact, there is a reasonably good linear correlation between the two, as shown in Figure 11c. These changes obviously reflect the influence of clay intercalation and exfoliation on the out-of-plane $Si-O^-$ mode. They are related to the changes in the distribution of environments of the $Si-O^-$ bonds, and as already mentioned, this distribution may take on some degree of asymmetry. Under the conditions used in this experiment, the intercalation seems to take place rather quickly, and an equilibrium state is reached within a few minutes.

Figure 12 shows two other parameters, based on peak areas, that are sensitive to the processing. To avoid any dependence on the overall spectral intensity, we use the ratio of peaks within the same spectrum. One parameter (Figure 12a) is the ratio of the area of peak III (the sum of IIIa and IIIb) against the area of peak IV. This ratio increases rapidly with processing for the first 5 min or so and then reaches a steady state. Again, the steady-state level seems to correlate with the Polybond concentration, although not quite as well as it does for the peak II position. The ratio of peak II to peak IV was also examined, but it did not change as much. It is worth repeating here that Yan et al.,[15] in their study of water swelling of montmorillonite, also found that the position of peak II and the ratio of peak III to peak IV varied in a manner similar to that seen here. Another parameter that is sensitive to the processing (Figure 12b) is the ratio of the area of the broad underlying peak V against the sum of peaks I to IV. It also changes rapidly within the first few minutes, although in this case it decreases as the band envelope narrows. It is interesting to note that in this case, although the initial rate of change depends on the Polybond concentration, the ultimate value reached is much less sensitive.

It would obviously be useful to have data from other techniques to support our conclusions. Although quantitative data on the state of intercalation/exfoliation are not readily available, the X-ray diffraction data obtained on our extruded samples do provide some support. The samples containing 2% Polybond or less all showed a clear intercalation peak. Samples with a high Polybond content, on the other hand, showed either no peak or only a very weak one, indicating a much better state of exfoliation. The corresponding *d*-spacing values determined where possible are given in Table 1. The *d*-spacing for the starting clay was 2.4 nm. Apart from somewhat anomalous values for the 2% Polybond sample, they follow a logical trend. For a recirculation time of 0 min (one pass through the extruder) they increase with Polybond concentration, from 3.08 nm at 0% to 3.48 nm at 100%. For 0% and 1% Polybond, they also increase with recirculation time, as expected, but only up to 5 min. Beyond this they appear to decrease, but there is a plausible explanation for this, namely that the clay stacks with larger *d*-spacings, corresponding to the low angle side of the peak, are being preferentially exfoliated, leaving behind the stacks with smaller spacings and thus shifting the peak maximum to

Table 1. Clay Interlayer Spacings (in nm) Determined by XRD for Extruded Samples of Blends of Polybond 3009 and HDPE Containing 2% Cloisite 20A

recirculation time (min)	Polybond content (%)					
	0	1	2	33	67	100
0	3.08	3.11	3.67	3.27	3.37	3.48
1	3.15	3.30	3.24			
2	3.27	3.34	3.15			
5	3.37	3.39				
10	3.04	3.08	3.14			
20	3.21	3.13	3.09			
30	3.16	3.48	3.53			

a lower *d*-spacing value. This underlines the problem of trying to correlate the peak maximum, which is a rather limited measure of the overall state of exfoliation, with the infrared data, which represents an average over the entire sample. In fact, infrared spectroscopy is probably the better technique for obtaining a complete and quantifiable measure of the state of intercalation. Furthermore, it has the potential to be applied as a relatively fast and easy quality control method. On-line application to polymer melts can also be envisaged, for example through the use of attenuated total reflection (ATR), and in fact our ongoing work is providing support for the potential of this approach.

Conclusion

The potential of infrared spectroscopy as a method for characterizing the state of intercalation/exfoliation in polymer nanocomposites containing montmorillonites has been clearly demonstrated. The shape of the clay absorption envelope at 1350−750 cm^{-1} changes as a function of processing, and this presumably results from better intercalation and exfoliation. This is supported by X-ray diffraction results. When peak fitting was applied to better understand the reasons for the changes, two main factors were identified. The first is a change in position and width of the peak arising from the out-of-plane $Si-O^-$ vibrational mode, both of which change with processing until a steady state is reached. The position of the peak in this steady state is dependent on the amount of compatibilizing agent present in the material. At this point it is not clear whether this is solely due to physical effects (increasing interlayer distance) or whether the chemistry of the compatibilizing agent also plays a role. The presence of a higher amount of polar maleic anhydride groups may result in enhanced interaction with the $Si-O^-$ dipoles. The second factor is a narrowing of the overall band envelope that may be represented (if somewhat empirically) by the diminishing contribution of a broad underlying peak. Our ongoing work indicates that similar changes occur in other polymers like polystyrene, polyamides, and epoxy resins. Other ongoing work is being devoted to other types of clays and to model studies in mineral oil in order to better understand the origins of these changes.

Acknowledgment. This work was supported by the members of the "PNC-Tech" industrial technology group, and we thank them for their support and the permission to publish. Thanks are also due to Ms. Dominique Desgagnés for her careful work in recording many infrared spectra, to Ms. Chantal Coulombe for the preparation of samples in the microextruder, and to Ms. Florence Perrin-Sarazin and Ms. Geneviève Dorval-Douville for supplying the blown PP films.

References and Notes

(1) Vaia, R. A.; Liu, W. *J. Polym. Sci., Part B: Polym. Phys.* **2002**, *40*, 1590−1600.
(2) Morgan, A. B.; Gilman, J. W.; Jackson, C. L. *Macromolecules* **2001**, *34*, 2735−2738.
(3) Drummy, L. F.; Koerner, H.; Farmer, K.; Tan, A.; Farmer, B. L.; Vaia, R. A. *J. Phys. Chem. B* **2005**, *109*, 17868−17878.
(4) Farmer, V. C. In *The Infrared Spectra of Minerals*; Farmer, V. C., Ed.; Mineralogical Society: London, 1974; Chapter 15, pp 331−363.
(5) Farmer, V. C.; Russell, J. D. *Spectrochim. Acta* **1964**, *20*, 1149−1173.
(6) Farmer, V. C.; Russell, J. D. *Spectrochim. Acta* **1966**, *22*, 389−398.
(7) Farmer, V. C.; Russell, J. D. In *Clay Mineralogy: Spectroscopic and Chemical Determinative Methods*; Wilson, M. J., Ed.; Chapman & Hall: London, 1994; Chapter 2, pp 11−67.
(8) Cole, K. C.; Perrin-Sarazin, F.; Dorval-Douville, G. *Macromol. Symp.* **2005**, *230*, 1−10.
(9) Ijdo, W. L.; Kemnetz, S.; Benderly, D. *Polym. Eng. Sci.* **2006**, *46*, 1031−1039.
(10) Farmer, V. C.; Russell, J. D. *Clays Clay Miner.* **1967**, *15*, 121−142.
(11) Russell, J. D.; Farmer, V. C. *Clay Miner. Bull.* **1964**, *5*, 443−464.
(12) Lerot, L.; Low, P. F. *Clays Clay Miner.* **1976**, *24*, 191−199.
(13) Zhang, Z. Z.; Low, P. F. *J. Colloid Interface Sci.* **1989**, *133*, 461−472.
(14) Yan, L.; Low, P. F.; Roth, C. B. *Clays Clay Miner.* **1996**, *44*, 749−756.
(15) Yan, L.; Roth, C. B.; Low, P. F. *Langmuir* **1996**, *12*, 4421−4429.
(16) Yan, L.; Roth, C. B.; Low, P. F. *J. Colloid Interface Sci.* **1996**, *184*, 663−670.
(17) Yan, L.; Stucki, J. W. *Langmuir* **1999**, *15*, 4648−4657.
(18) Schaefer, F. W.; Wright, A. C.; Granquist, W. T. *NLGI Spokesman* **1971**, *34*, 418−423.
(19) Cole, K. C.; Pilon, A.; Noël, D.; Hechler, J.-J.; Chouliotis, A.; Overbury, K. C. *Appl. Spectrosc.* **1988**, *42*, 761−769.
(20) Heuvel, H. M.; Huisman, R.; Lind, K. C. J. B. *J. Polym. Sci., Polym. Phys. Ed.* **1976**, *14*, 921−940.
(21) Heuvel, H. M.; Huisman, R. *J. Appl. Polym. Sci.* **1985**, *30*, 3069−3093.
(22) Loo, L. S.; Gleason, K. K. *Macromolecules* **2003**, *36*, 2587−2590.
(23) Romeo, M.; Mohlenhoff, B.; Diem, M. *Vib. Spectrosc.* **2006**, *42*, 9−14.

MA0628329